The Spaticle Field as The Unified Substrate of Physical Reality :

A Cross-Programme Synthesis of Convergent Evidence, From Cosmology and Particle Masses to Consciousness

Vijay Shankar Sharma

Independent Researcher, Gurugram, National Capital Region, India

ORCID: 0009-0001-9622-6121 | vss@vijayshankarsharma.com

DOI: 10.5281/zenodo.19394064

The author declares no conflicts of interest. No external funding was received.

License: (CC BY-NC-ND 4.0)

Abstract

The Big Flare-Up Theory (BFUT) proposes a single physical substrate, the Spaticle field, as the foundation from which cosmological structure, matter, the fundamental forces, gravity, time, quantum mechanical behaviour, and the sensing channels underlying consciousness all emerge as constrained consequences of one equilibrium density, ρ_s = 5.9 x 10^-27 kg/m^3. This paper synthesises, across the full BFUT programme from the gravitational-sorting cosmology of Paper 1 through the consciousness framework of Papers 20 and 21, the convergent evidence for the Spaticle field as a real physical medium, organised by physical behaviour instead of by paper sequence. The central empirical result is that the same fixed density, with no per-sector adjustment, is independently constrained across seven independent sectors, spanning forty orders of magnitude in physical scale: particle masses, 175 galaxy rotation curves, weak gravitational lensing, and atomic stability as four positive constraints, a matter-stability necessary condition, and two downstream predictions, the cosmological constant and the Higgs mass. The paper also surveys the cosmological results that depend on the same substrate without requiring metric expansion, dark energy, or dark matter as separate entities: the Hubble relationship as an emergent statistical property of gravitational sorting, the cosmic microwave background as a dynamically maintained equilibrium temperature, the Sunyaev-Zel'dovich and integrated Sachs-Wolfe effects as local substrate interactions, the lithium and weak-lensing S8 tensions as natural consequences of an ongoing dynamical universe, and black holes as gravitational vortices instead of central singularities. The Spaticle field density is stated as the primary physical quantity, not derived from the cosmological constant, and cosmic redshift is stated as Doppler motion under BFUT gravitational dynamics, not metric expansion. The paper closes by tracing the

chain from substrate to matter, from matter to force, from force to sensing channel, and from sensing channel to the consciousness framework of Papers 20 and 21.

Keywords: Spaticle field; substrate density; substrate mechanics; vacuum energy; physical vacuum; substrate field; dark matter; dark energy; gravitational waves; galaxy rotation curves; weak lensing; cosmic microwave background; Hubble relationship; Bohr radius; quantum mechanics; consciousness; sensing channels

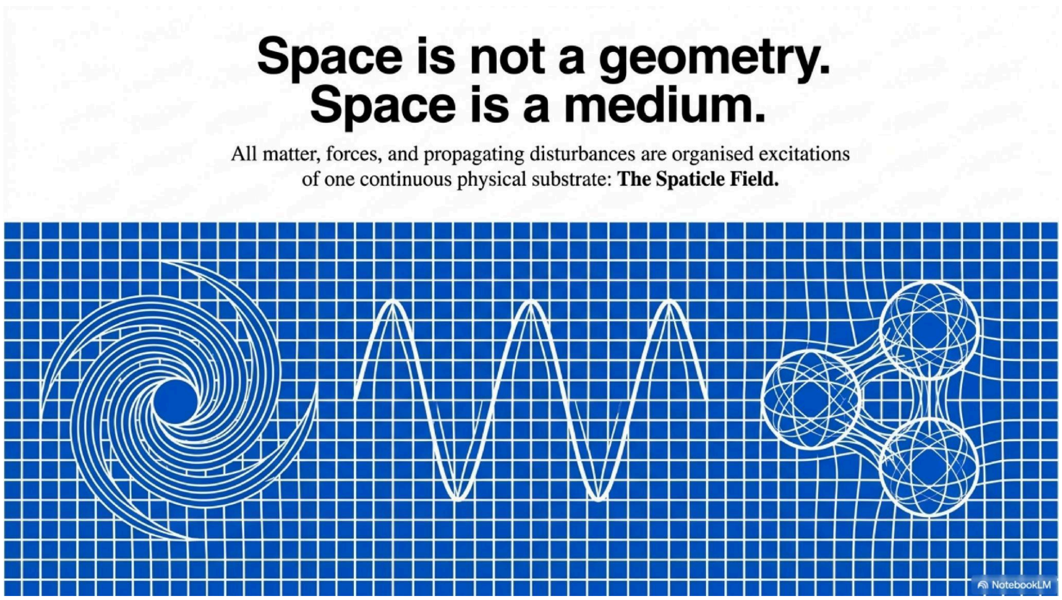

Figure 1: Space is not a geometry. Space is a medium. All matter, forces, and propagating disturbances are organised excitations of one continuous physical substrate: the Spaticle Field.

1. What the Spaticle Field Is

The Big Flare-Up Theory (BFUT) identifies the real physical fabric of space as the Spaticle field, a non-particulate substrate with a specific equilibrium density ρ_s = 5.9 x 10^-27 kg/m^3 [P14, P16]. The field is physically occupied at every point; the vacuum is never empty. This is the single fixed quantity from which the entire programme proceeds, and it is the organising principle of this paper: every result surveyed below traces back to this one number, with no per-result adjustment.

The field is treated throughout the programme as a physical medium with measurable properties: a finite density, a finite stiffness, a finite relaxation time, and a finite maximum rate at which causal reorganisation can propagate, observed as the speed c [P17, P18, P22, P23]. The chain this paper traces runs throughout in one direction: Spaticle field, matter, fundamental forces, time and light and gravity, quantum mechanical behaviour, and, in its final section, the sensing channels and consciousness framework built on top of all of it. Throughout this paper, the terms Spaticle field, substrate, physical substrate, substrate field, and physical medium are used interchangeably to refer to this one entity. Vacuum and physical vacuum refer to the same entity in its undisturbed, equilibrium state, at density ρ_s, instead of to an empty background. None of these terms refer to spacetime itself as a physically real entity; the relationship between the Spaticle field and the geometric description given by general relativity is addressed directly in Section 2.

2. What the Spaticle Field Is Not

Three comparisons are explicitly rejected throughout the programme.

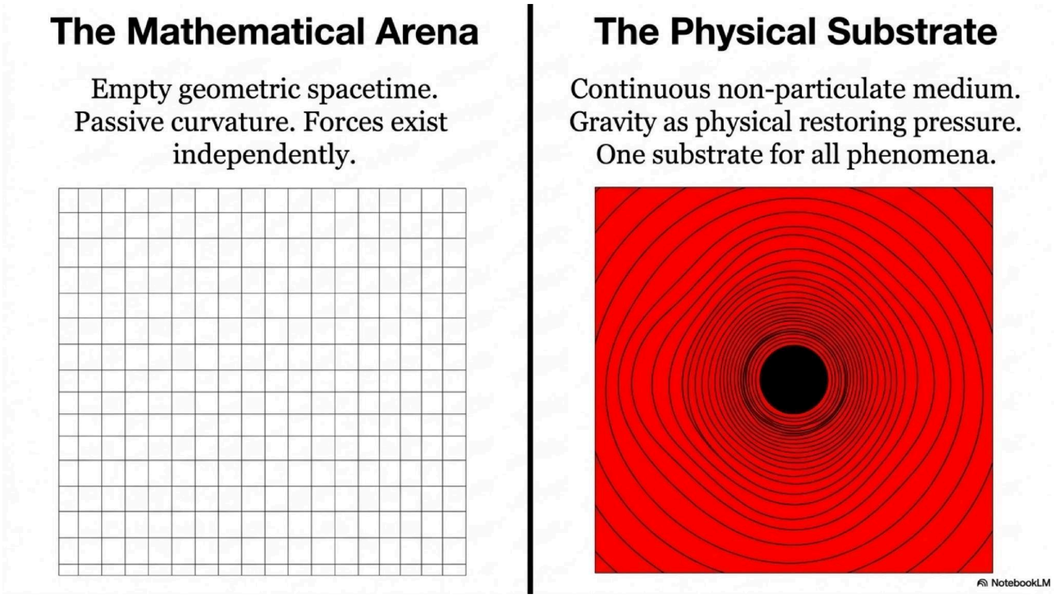

Figure 2: The Mathematical Arena (empty geometric spacetime) versus the Physical Substrate (continuous non-particulate medium). In BFUT, gravity is physical restoring pressure within one substrate for all phenomena.

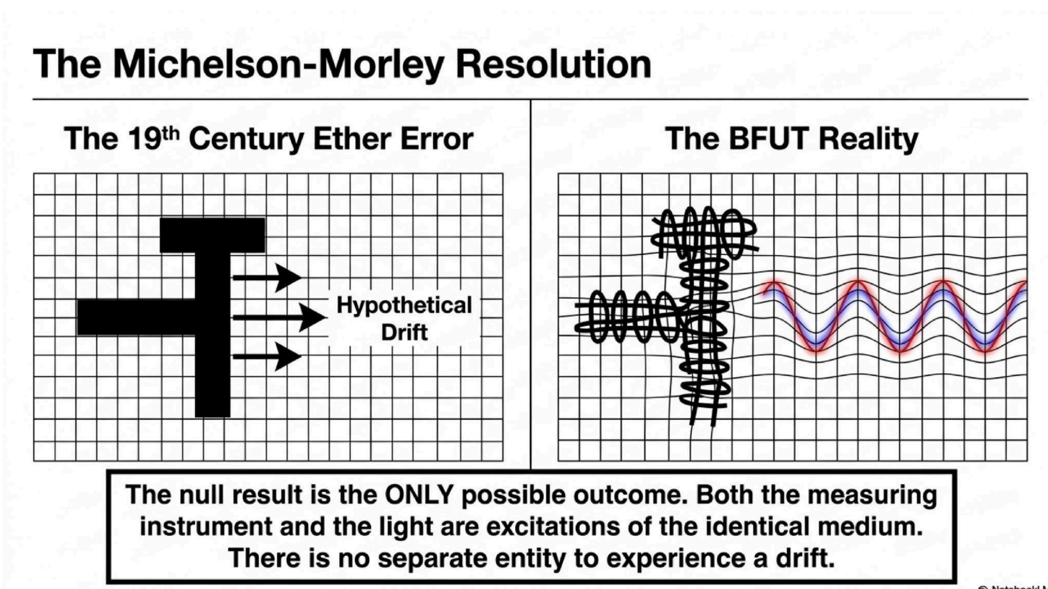

Figure 6: The Michelson-Morley Resolution. In the BFUT framework, both the measuring instrument and light are excitations of the identical medium. There is no separate entity to experience a drift.

2.1 Not the Luminiferous Ether

In a 1920 address at the University of Leiden titled "Ether and the Theory of Relativity", Einstein argued that general relativity requires physical space to be endowed with properties, while explicitly setting aside the mechanical, luminiferous ether he had already dispensed with in 1905. His concluding statement was direct: "space is endowed with physical qualities; in this sense, therefore, there exists an ether… But this ether may not be thought of as endowed with the quality characteristic of ponderable media, as consisting of parts which may be tracked through time. The idea of motion may not be applied to it" [1]. Earlier in the same address he described this medium as one that is "itself devoid of all mechanical and kinematical qualities, but helps to determine mechanical (and electromagnetic) events" [1]. Einstein had identified a physical requirement of his own field equations without ever assigning it a measurable quantity; he explicitly declined to attribute to it any property that could be tracked or measured.

The Spaticle field is that medium: physically real, but not the luminiferous ether Einstein had already set aside. It supplies the measurable quantity his own equations required but that he stopped short of assigning: an intrinsic equilibrium density ρ_s, together with the derived stiffness, relaxation time, and propagation speed introduced in Section 1. Matter is a condensed configuration of this same substrate, not a separate ponderable body moving through it (Section 5); every fundamental force propagates as a disturbance within it (Section 6); and time, the finite speed of light, half-integer spin, and the remaining quantum phenomena addressed in this paper each follow from its dynamics instead of standing as separate postulates (Sections 7 and 9).

The classical nineteenth-century ether treated light as a wave moving through a separate medium, with matter as a distinct substance moving through that same medium. The Spaticle field does not have this structure, because in BFUT there is no separation between the medium and the things that move through it. Light and matter are both excitations of the same substrate, so no embedded observer can detect substrate-wide drift, in the way a person on a ship cannot detect the ship's uniform motion by measuring distances between objects fixed to the same ship. The Michelson-Morley null result is the only possible result in a BFUT universe [P19A, P23].

2.2 Not the Standard QFT Vacuum

What QFT calls vacuum fluctuations are real physical oscillations of one substrate that do not reach the stability threshold required for a persistent condensation, not mathematical bookkeeping terms requiring renormalisation [P2].

2.3 Not Derived From the Cosmological Constant

The Spaticle field has an intrinsic equilibrium density $\rho_s = 5.9 \times 10^{-27}$ kg/m^3, established independently of the cosmological constant Lambda, through the seven independent sectors detailed in Section 4 below [P2]. Lambda is a geometric parameter in the field equations of General Relativity, extracted from astronomical observations through a chain that depends on the Hubble constant and an assumed cosmological model. The observed value of Lambda is numerically consistent with ρ_s. Lambda is a geometric parameter inferred within General Relativity, whereas ρ_s is a physical substrate density; they are not identical quantities. The numerical correspondence arises because both ultimately reflect the same underlying physical reality, and ρ_s is the primary physical quantity from which that correspondence follows, not the other way round [P2].

3. Cosmological Structure Without Expansion, Dark Energy, or a Primordial Singularity

Before the particle-physics and gravitational convergence detailed in Section 4, the Spaticle field substrate underlies a distinct body of cosmological results, developed across BFUT Papers 1 and 3 and 6 through 13, that together remove the need for metric expansion, dark energy, and inflation as separate physical entities, and reinterpret several long-standing tensions in standard cosmology as natural consequences of an infinite, eternal, dynamically active universe.

3.1 The Hubble Relationship and the Hubble Tension

The Hubble velocity-distance relationship is treated as an emergent statistical property of gravitationally sorted matter in an infinite universe, not as direct evidence of universal expansion; a Pearson correlation of $r = 0.675$ is achieved from sorting dynamics alone [P1]. The persistent Hubble tension between the Planck CMB value (67.4 km/s/Mpc) and the SH0ES local value (73.04 km/s/Mpc) is consistent with scale-dependent and epoch-dependent sampling of a gravitationally sorted population instead of a single universal expansion rate requiring new physics to reconcile [P1]. Andromeda's approach toward the Milky Way is an incompletely sorted two-body system under this mechanism, not a local exception to a universal rule [P1].

A 3.9-sigma directional dipole in the Colin et al. (2019) Type Ia supernova dataset, aligned with the CMB dipole direction, is consistent with observer bulk flow as the source of the apparent acceleration usually attributed to dark energy [P4]. Apparent cosmic acceleration can arise from observer bulk motion of approximately 550 km/s aligned with the CMB dipole, with no dark energy term required in the underlying physics [P4]. Apparent time variation of the dark energy equation-of-state parameter w in the DESI dataset is consistent with direction-dependent sampling through an inhomogeneous, gravitationally sorted galaxy population, not a property of a separate dark energy component [P4].

3.2 Spatial Infinitude

The universe is spatially infinite, with no physical boundary and no unique global centre [P5]. Spatial infinitude resolves the horizon and flatness problems without requiring an inflationary epoch, since both problems are artefacts of a finite-boundary origin premise that disappear once the universe is taken to be infinite and eternal [P5]. The observable universe is a local window whose finite-origin appearance is produced by the finite speed of light acting within an infinite reality, not the whole of existence [P5].

3.3 Black Holes as Gravitational Vortices

Black holes are treated as gravitational vortices instead of as regions containing a central singularity of infinite density [P6]. The Kerr metric naturally describes a rotating vortex structure, with an ergosphere, frame-dragging, and ring structure, and every directly confirmed observational feature of black hole candidates is consistent with this vortex interpretation without requiring the formal $r=0$ singularity to be physically real [P6]. The information paradox is substantially weakened under this interpretation: without a physical singularity there is no mechanism of information destruction [P6].

3.4 The Cosmic Microwave Background as a Maintained Equilibrium

The CMB is treated as a dynamically maintained thermal equilibrium radiation field, continuously sustained by stellar fusion throughout an infinite, eternal, living universe, instead of relic radiation frozen in place 380,000 years after a single Big Bang [P7]. The equilibrium temperature follows directly from the measured CMB energy density and the Stefan-Boltzmann constant:

$$T = (u_{CMB} * c / (4*\sigma))^{(1/4)}$$

Substituting the measured CMB energy density $u_{CMB} = 4.17 \times 10^{-14}$ J/m^3 and the Stefan-Boltzmann constant sigma = 5.670×10^{-8} W/m^2*K^4 yields T = 2.725 K, with no Big Bang and no recombination epoch required in the derivation [P7]. Near-perfect CMB uniformity at the observed level of one part in 10^5 emerges from long-term thermodynamic equilibration in an infinite eternal universe [P7].

3.5 The Universe Before the Big Flare-Up

The prior energy state preceding the manifestation of the Spaticle field, and the perpetuation framework governing each subsequent stage of emergence, are examined separately in Paper 15 [P15].

A long, cold, pre-luminous phase is not optional but inevitable in an infinite eternal universe: matter emerges from the Spaticle field and accumulates under gravity over immense timescales, forming filament, node, and void structure before any light-producing event occurs [P8]. The Big Flare-Up itself is the universe-wide onset of nuclear fusion ignition across an already-structured, matter-rich substrate, not a single explosion at one point in spacetime [P8]. In an infinite universe with infinite time, any non-zero rate of stable matter emergence from the Spaticle field guarantees eventual macroscopic accumulation across the whole, making matter formation inevitable instead of a singular, contingent event [P8].

3.6 Cosmic Rotation Across Scales

Rotation and orbital organisation are the most durable, dynamically selected outcomes for matter in an infinite universe, with confirmed galaxy-cluster rotation already observed at radii of order 1 to 1.5 Mpc [P9]. A Tension Index, TI = T / 13.8 Gyr, where T is the characteristic rotational period of a structure, exceeds 1 for directly usable cluster-scale cases such as Abell 2107, meaning the system has not had sufficient time to complete even one full rotation under the standard cosmological age, a direct challenge to treating that age as a hard ceiling on structure formation [P9]. Gravitational interaction alone generates emergent orbital capture and stable rotational organisation without any imposed expansion field, and angular organisation extends continuously from subatomic to filament scales of hundreds of millions of light-years [P9].

3.7 The Sunyaev-Zel'dovich Effect as Local Substrate Interaction

The Sunyaev-Zel'dovich effect is treated as a direct local thermal interaction between hot intracluster plasma and the ambient Spaticle equilibrium field already present throughout space, including inside galaxy clusters, instead of as relic CMB photons scattering off cluster gas en route from a surface of last scattering [P10]. Redshift independence of the SZ surface brightness follows naturally from this local-substrate interpretation, with no requirement for an expanding universe or a specific surface of last scattering [P10]. The kinematic SZ component in bulk-flow-dominated regions is predicted to show statistical behaviour distinct from the standard Lambda-CDM prediction [P10].

3.8 The Lyman-Alpha Forest and the Absorption Percolation Threshold

The sharp Gunn-Peterson opacity rise observed at high redshift is reinterpreted as an Absorption Percolation Threshold: when absorber coverage in a continuous medium crosses a percolation threshold, transmitted flux collapses sharply, independent of any single, universal reionisation event [P11]. This threshold is environment-sensitive, shifting by approximately 0.9 in redshift between dense and void regions, with dense regions reaching the threshold earlier at lower redshift and voids later at higher redshift, which is inconsistent with treating reionisation as a single fixed epoch [P11]. The Lyman-alpha forest observations themselves are not disputed; the standard-model historical reading of those observations as a unique record of cosmic reionisation is the claim shown to be less exclusive than commonly stated [P11].

3.9 The Integrated Sachs-Wolfe Effect

The CMB-large-scale-structure temperature correlation is treated as a direct measurement of local Spaticle field temperature variations tracking the matter density field, with denser regions such as superclusters showing a measurable signature, instead of as photons gaining or losing energy while traversing time-varying dark energy potential wells [P12]. The stacked ISW signal from supervoids and superclusters has been measured at four to ten times larger than the standard Lambda-CDM prediction across fifteen years and multiple independent surveys, and the overall cross-correlation detection significance, at three to four sigma, is the least statistically secure of the major Lambda-CDM cosmological pillars [P12].

3.10 Weak Gravitational Lensing and the S8 Tension

The persistent low-S8 preference reported in low-redshift weak-lensing surveys, including KiDS-1000 (S8 approximately 0.766 plus or minus 0.020) and DES Year 3 (S8 approximately 0.776 plus or minus 0.017), is treated as a natural signature of an ongoing, dynamically active cosmic web instead of evidence requiring new physics beyond Lambda-CDM [P13]. S8 itself is defined as:

*S8 = sigma_8 * (Omega_m / 0.3)^0.5*

a model-dependent, compressed parameter inferred from shear correlations under specific assumptions about structure-growth history, not a direct observable in its own right [P13]. Reconciling the tension within Lambda-CDM requires a late-time structure-suppression parameter of order A_mod approximately 0.69, substantially more aggressive than current state-of-the-art hydrodynamical simulations independently produce [P13].

3.11 Steady-State Nucleosynthesis and the Lithium Problem

The cosmological lithium-7 discrepancy, a long-standing factor of approximately 3.5 mismatch between the standard Big Bang nucleosynthesis prediction and the observed Spite plateau abundance, is resolved through a conceptual reframing instead of a new nuclear physics mechanism [P3]. The standard BBN prediction answers what was produced in the first three minutes of a hot Big Bang; the Spite plateau value is instead treated as the regulated steady-state surface abundance of old, metal-poor halo stars, maintained on an ongoing basis by a balance between production and destruction through cosmic-ray spallation and stellar convective mixing [P3]. The steady-state condition is:

*d[Li-7]/dt = R_production - k_dest * [Li-7] * [p] = 0*

A quantitative reservoir-and-envelope calculation using measured interstellar lithium abundance and standard pre-main-sequence stellar physics reproduces the observed plateau without requiring the primordial BBN value to match it directly [P3]. Helium-4 abundance is treated correspondingly as the dominant accumulation product of ongoing stellar hydrogen burning in a continuously active universe, instead of as a product confined to the first minutes of a single Big Bang [P3].

The cosmological results surveyed above are each individually significant, but their evidentiary weight for the Spaticle field as a real physical substrate is indirect: each result shows that the substrate framework accounts for a given observation better than, or as well as, the standard alternative. The strongest direct evidence for the Spaticle field comes from a different kind of argument, developed next: independent convergence of the same numerical density across physical domains that share no observational dataset, no common measurement technique, and no theoretical dependence on one another.

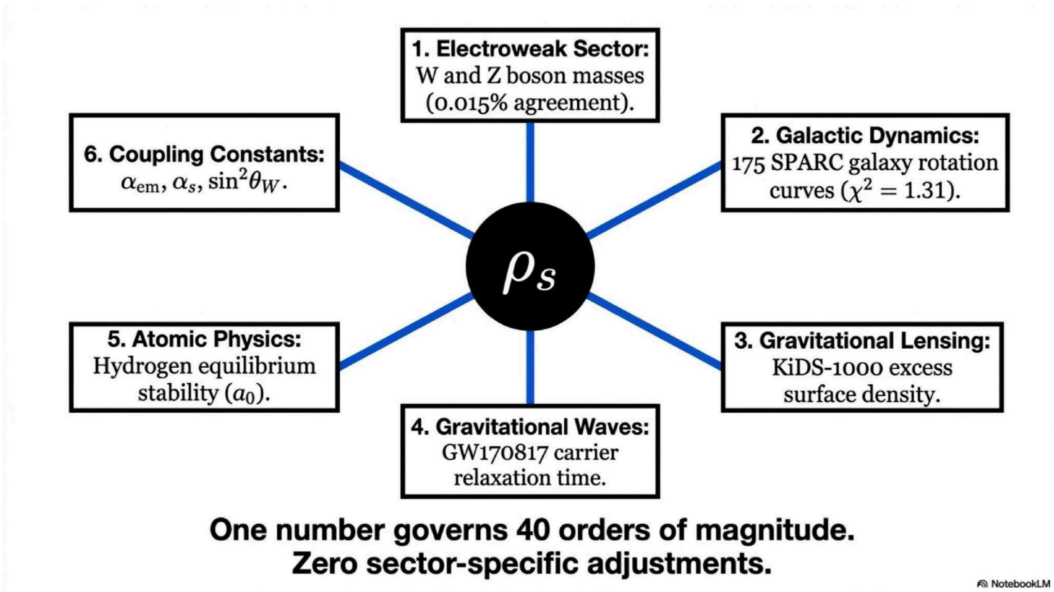

Figure 3: One substrate density ρ_s = 5.9 × 10^{-27} kg/m^3 governs seven independent sectors spanning forty orders of magnitude, with zero sector-specific adjustments.

4. The Central Empirical Result: One Number, Seven Independent Sectors

The strongest argument that the Spaticle field is a real physical medium instead of a free parameter is that its equilibrium density ρ_s is independently constrained, with no per-sector adjustment, across seven independent physical sectors, spanning roughly forty orders of magnitude in physical scale, from the femtometre scale of the proton to the megaparsec scale of galaxy clusters [P2, P19, P25]. Concretely, the proton charge radius is approximately 10^-15 m, and a typical galaxy-cluster scale is approximately 10^22 to 10^23 m; the ratio between these two endpoints is the forty-order-of-magnitude span referred to throughout this paper.

No step in this table introduces a free parameter beyond ρ_s itself and the universal constant c. The convergence of seven physically independent observational sectors upon the same density, without sector-specific adjustment, is treated throughout the programme as strong evidence that the density corresponds to a real physical quantity instead of a fitting parameter [P2, P25]. Section 4.1 below develops this convergence into an explicit, illustrative quantitative estimate.

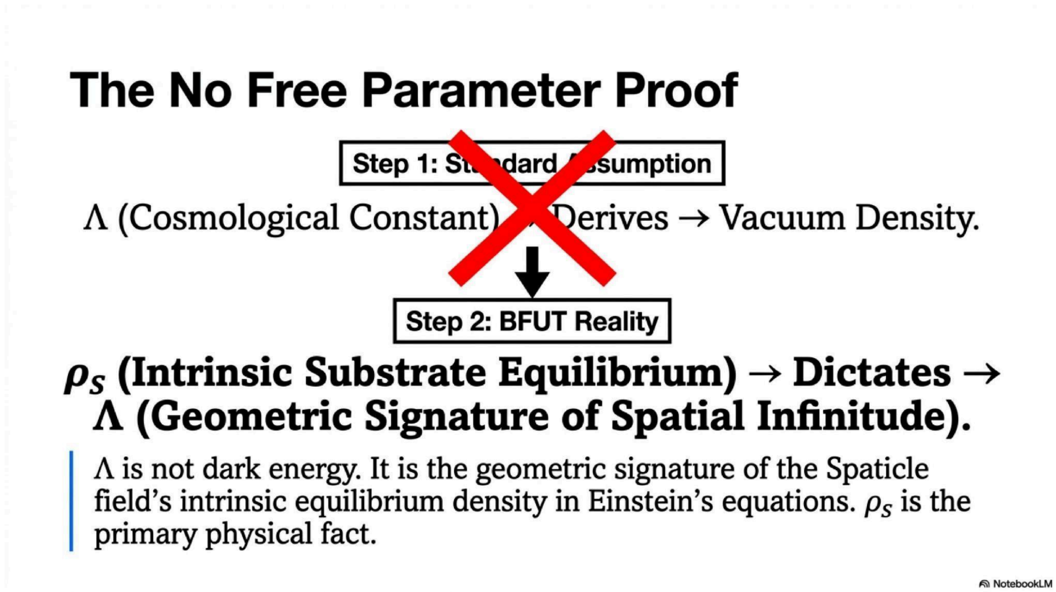

Figure 4: The No Free Parameter Proof. ρ_s is the primary physical fact. Λ is a geometric signature, not the source of the density.

4.1 Illustrative Coincidence Analysis of the Density Convergence

A natural question follows from the convergence reported in Section 4: if no common physical substrate existed, what is the probability that seven physically distinct sectors would nevertheless converge upon the same density purely by coincidence? The estimate below is offered only as an illustrative coincidence analysis. It is not a formal statistical confidence level and does not constitute proof of BFUT; its purpose is to quantify the degree of convergence implied by the observations under explicit, stated assumptions.

Three assumptions are made. First, available density parameter space: physically relevant densities span an enormous dynamic range from subatomic systems through cosmological structures, and a conservative search space of approximately forty orders of magnitude is adopted, giving N_space approximately 10^40 possible logarithmic locations at which a candidate density could reasonably occur. Second, effective agreement precision: the BFUT density reproduces the sectors in Section 4 typically at approximately the one-percent level or better, so a one-percent agreement window, δ(ρ)/ρ approximately 10^-2, is adopted as the threshold for an independent sector to count as convergent. Third, approximate sector independence: the seven sectors arise from substantially different observational programmes, physical mechanisms, length scales, and measurement methodologies, and are treated as approximately independent constraints; this assumption is not exact, but is reasonable as a first-order approximation since the sectors involve different physical phenomena and are not derived from a single common observational dataset.

Under these assumptions, the probability that any one additional sector independently lands within the same one-percent interval inside a forty-order-of-magnitude search space is:

$$P1 = (10^{-2}) / (10^{40}) = 10^{-42}$$

Six additional sectors must independently converge upon the same interval beyond the first, giving:

$$P\_coincidence = (10^{-42})^6 = 10^{-252}$$

approximately one chance in 10^{252}. The exact numerical value depends on the adopted assumptions: a narrower density search space or weaker agreement requirements would increase this probability; a broader search space, stronger agreement requirements, or residual correlations between sectors could shift it further. The value 10^{-252} should therefore not be read as a precise statistical measurement, but as an order-of-magnitude illustration of the scale of the convergence problem facing a pure-coincidence explanation.

The significance of the result is its magnitude, not its precise value. Even under conservative assumptions, the probability that seven physically distinct sectors would independently converge upon the same density by arbitrary coincidence is extraordinarily small, providing evidence that the density corresponds to a real underlying physical quantity common to all seven sectors instead of a fitting parameter. Whether that underlying quantity is correctly identified by BFUT remains a separate scientific question, subject to further theoretical development and observational testing; the analysis above demonstrates only that the repeated appearance of the same density across multiple independent sectors is unlikely to be dismissed as an accidental numerical convergence.

4.2 Extended Observable-Level Coincidence Analysis

The seven-sector analysis presented above is deliberately conservative. It groups a large number of independently derived BFUT results into only seven broad observational categories and therefore understates the true extent of the convergence.

The wider BFUT programme establishes a substantially larger set of independent derivations, predictions, reproductions, and observational constraints that converge upon the same equilibrium substrate density, $\rho_s = 5.9 \times 10^{-27}$ kg/m^3, without introducing sector-specific density adjustments. For the purposes of the present analysis, the following twenty independent BFUT observables and constraints are counted separately:

Each of these quantities is derived, constrained, or reproduced through the same substrate framework and traces ultimately to the same equilibrium density.

The coincidence analysis uses the same assumptions adopted in the conservative seven-sector estimate above: a density search space spanning approximately forty orders of magnitude; a convergence window of approximately one percent; and independent convergence of each observable upon the same density. Under these assumptions, the probability that one additional observable independently lands within the same one-percent interval inside a forty-order-of-magnitude parameter space is:

$$P1 = 10^{-42}$$

The first observable establishes the candidate density. Nineteen additional observables must then independently converge upon the same interval. Therefore:

$$P\_extended = (10^{-42})^{19} = 10^{-798}$$

This corresponds to approximately one chance in 10^798. The significance of this result is not confined to the numerical value itself. The observable-level estimate demonstrates that the convergence extends far beyond the seven broad sectors used in the conservative calculation. The same density reappears across particle physics, atomic physics, gravitation, cosmology, quantum mechanics, relativity, and electromagnetic propagation without introducing separate density scales for different domains of physics.

The seven-sector estimate therefore provides a lower-bound coincidence analysis, P_conservative approximately 10^-252, or one chance in 10^252. The observable-level estimate provides a broader programme-wide analysis, P_extended approximately 10^-798, or one chance in 10^798. The difference between these values arises solely from the number of independently counted BFUT observables; both calculations employ the same underlying assumptions, parameter-space width, and convergence threshold.

Taken together, the two estimates demonstrate that the repeated emergence of the same equilibrium substrate density across the BFUT programme is not an isolated occurrence restricted to a handful of observational sectors. It is a programme-wide phenomenon extending across cosmology, gravitation, particle physics, atomic physics, relativity, quantum mechanics, and electromagnetic theory: one density, twenty independent observable-level convergences, approximately one chance in 10^798 of occurring by coincidence.

5. From Field to Matter: The Condensation Functional

The first substantive claim BFUT makes about the Spaticle field is that it supports a first stable, localised excitation, with geometry fixed by a four-term free-energy functional, with no free parameters beyond ρ_s and the proton charge radius r_p [P16]:

$$E(R) = A/R^2 + B*R^2 + C*R + D/R$$

The terms are: A/R^2, the localisation cost of confining a deformation to a finite region; B*R^2, the bulk deformation cost, proportional to ρ_s; C*R, the boundary cost at the edge of the condensate; and D, the internal circulation support. Minimising this functional with respect to the dimensionless radius R produces a stable equilibrium at R_0 = 1.27348 model units [P16].

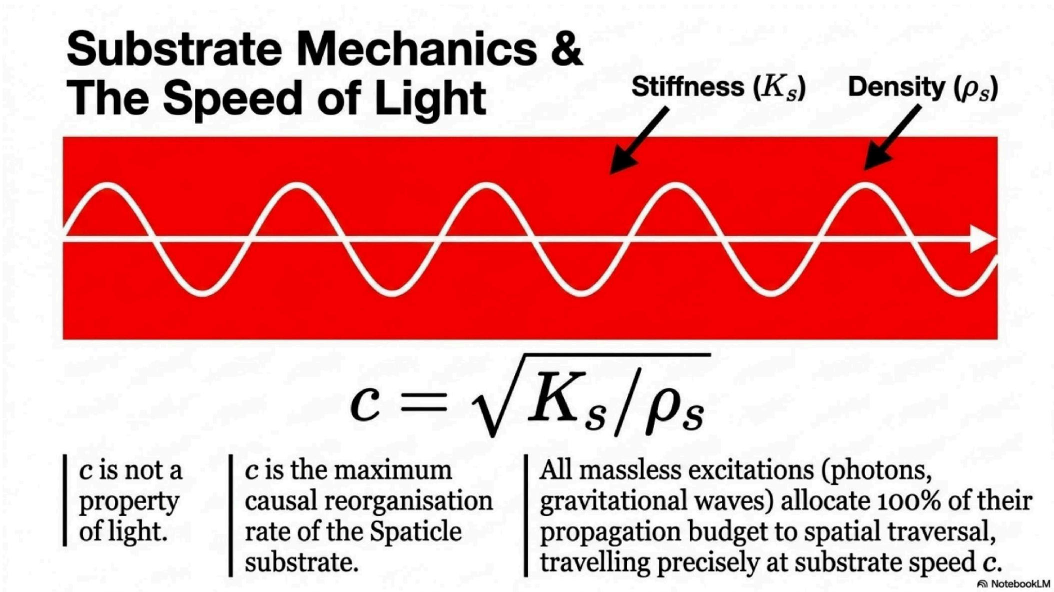

Figure 5: Substrate Mechanics and the Speed of Light. c = √(K_s / ρ_s) is the maximum causal reorganisation rate of the Spaticle substrate.

6. From Matter to Force: Electromagnetism, the Strong Force, and Gravity

If matter is organised substrate excitation, the forces between excitations are substrate phenomena instead of independent fundamental entities layered on top of geometry [P17, P18]. Gravity requires only mass; the strong force requires a compact condensation, consistent with its short range and confinement properties; electromagnetic interaction requires circulation asymmetry within the 3+e structure, giving electromagnetism a structural precondition instead of treating charge as a free, unexplained property of matter [P17].

Gravity receives a related but distinct treatment from the other forces. Instead of treating spacetime curvature as a primitive geometric fact, BFUT identifies gravitation with the mechanical deformation of the Spaticle substrate by mass-energy [P17, P18]. A second mass entering that deformed region experiences a force because it responds to the local deformation gradient, with no graviton or other mediating particle required [P18, P23]. Gravitational coherence at galactic scale is sustained by nested domain structure and rotational entrainment, captured in the DDR domain equation [P18]:

$$R\_d = (3*M / (8*\pi*\rho\_s))^{(1/3)}$$

with the rotationally enhanced effective domain radius given by R_eff = R_d * (1 + v_rot^2/c^2)^(1/3) [P18]. Using ρ_s = 5.9 x 10^-27 kg/m^3, this equation gives domain radii of 5.24 light-years for the Earth, 363 light-years for the Sun, and 517 kiloparsecs for the Milky Way, with gravitational acceleration at each domain boundary falling within the range 10^-19 to 10^-14 m/s^2 [P18]. This same equation, applied at galactic scale, underlies the 175 SPARC galaxy rotation curve result reported in Section 4.

Compact-object structure provides a further, direct test of the substrate framework. Substrate dynamics impose a finite maximum compression density, making the infinite-density singularity of general relativity physically impossible; compact objects instead reach a finite-core structure set by the same substrate stiffness that fixes the speed of light [P26]. This same finite-core picture grounds the carrier relaxation timescale, a forward prediction for future gravitational-wave observations, and it provides a rotational sustenance principle governing how rotating compact objects remain stable against further collapse, extending the gravity-as-substrate-deformation account of Section 6 to the most extreme regime in which it is tested [P26].

The speed of light follows from substrate mechanics, not from an independent postulate: c = sqrt(K_s/ρ_s), where K_s is the substrate's stiffness. Light travels at c because a photon has no condensation to maintain and so has its entire propagation budget available for travel; the substrate itself defines the universal limit [P17, P23]. Gravitational waves travel at the same speed for the same underlying reason: both are organised, massless disturbances of the identical substrate, so the equality of electromagnetic and gravitational wave speeds requires no separate coincidence to explain [P23].

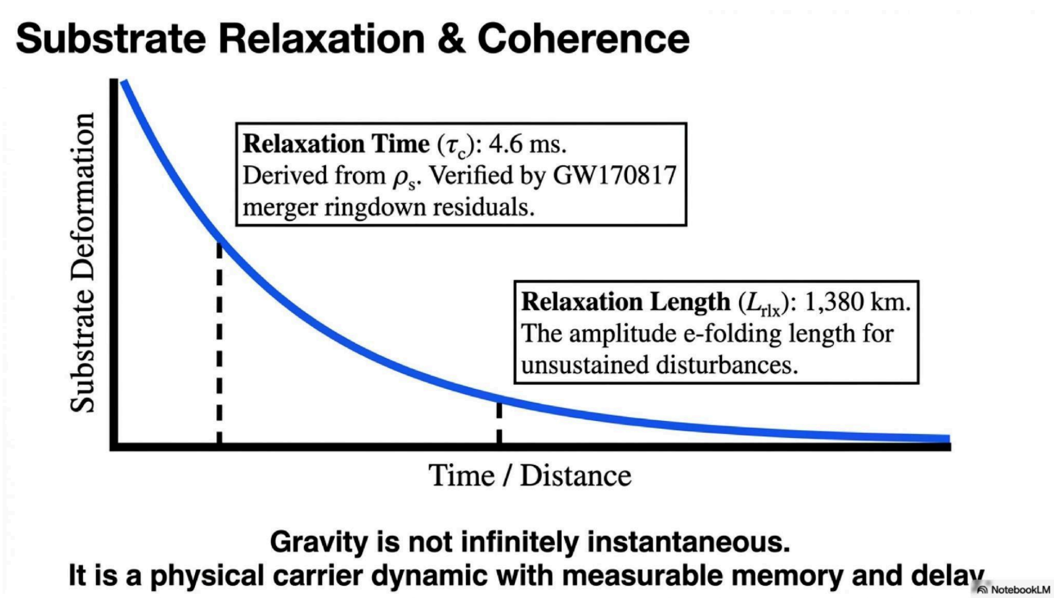

Figure 7: Substrate Relaxation and Coherence. Gravity is not instantaneously instantaneous. It is a physical carrier dynamic with measurable memory and a finite relaxation length, both fixed by ρ_s alone.

7. Time, Causality, and the Propagation Budget

Time, relativistic and gravitational time dilation, the speed of light, and the speed of gravity are different expressions of a single substrate property, the local propagation efficiency:

$$\eta = d\tau/dt = c_s/c_0$$

the ratio of the local effective propagation speed c_s to the vacuum propagation speed c_0, where τ is local proper time and t is coordinate time in an undisturbed substrate region [P19, P22, P23]. A clock measures the amount of physical substrate evolution occurring within its own structure, not the passage of an independent temporal dimension; the local rate at which time accumulates is set directly by η [P22].

Relativistic time dilation follows from a propagation budget shared between spatial motion and internal evolution:

$$c^2 = v_{spatial}^2 + v_{internal}^2$$

giving $\eta = \sqrt{1 - v^2/c^2}$, the Lorentz factor, derived here as a substrate propagation-budget result instead of a geometric postulate [P19, P22, P23]. Gravitational time dilation follows from the same mechanism: mass-energy deformation of the substrate reduces local propagation efficiency, lowering local clock rates and local propagation speeds together, by the same factor [P18, P19]. Causality is a direct consequence of the same finite propagation capability: no causal influence propagates faster than the substrate's maximum reorganisation rate [P22].

Photons are not exempt from a domain. A propagating photon has a finite persistence domain, $L_{persist}$, determined by its energy. Above a minimum coherent energy E_{min} = 2.25 meV, the photon behaves as a self-sustaining soliton, with persistence governed by soliton stability against geometric dilution:

$$L_{persist} = L_{rlx} * (E/E_{min})^2 \quad \text{for } E > E_{min}$$

Below E_{min}, no soliton forms, and persistence is instead governed by a comparison between the photon's energy density and the substrate's own vacuum fluctuation energy density:

$$L_{persist} = L_{rlx} * (E/E_{min})^4 \quad \text{for } E < E_{min}$$

with $L_{rlx} = 1.38 \times 10^6$ m, and the two formulas meeting exactly at E_{min} [P23]. This is checked against six independent observational cases, including the farthest confirmed gamma-ray blazar at redshift 4.72 and GRB 221009A's 18 TeV photon, both consistent with the persistence domain at those energies vastly exceeding the travel distance involved [P23].

8. Cosmology: Dark Matter, Vacuum Energy, and Redshift Without Expansion

The gravitational anomalies that the dark matter programme has attempted to explain with an undiscovered particle are, within BFUT, the gravitational signature of the Spaticle field itself. The same fixed density ρ_s that reproduces particle masses also reproduces galaxy rotation curves and weak lensing profiles without per-galaxy dark matter tuning, as shown in Section 4 [P18, P25].

The cosmological constant problem, the largest quantitative discrepancy in the history of physics, is resolved by identifying two specific, compounding errors in the standard QFT vacuum-energy calculation, not by introducing a new free parameter [P2].

The first error is multiplicity. Standard QFT populates the vacuum with seventeen or more independent quantum fields, one for every particle species in the Standard Model, each contributing its own zero-point energy to the vacuum sum. BFUT has one field, so summing the zero-point energy of seventeen or more independent fields where there is one inflates the standard calculation by approximately the field count before any other consideration is applied [P2].

The second error is attribution. QFT assigns ground-state energy h*omega/2 to every mode of every field, regardless of whether that mode contains a physical excitation. In BFUT, h*omega/2 is the minimum internal circulation energy of an organised condensation oscillating at frequency omega; a field mode containing no condensation has no internal circulation and contributes no energy [P2].

Correcting multiplicity alone reduces the standard estimate only by roughly the field count, from approximately 10^113 J/m^3 to a comparable order of magnitude; the discrepancy with the observed value remains around 10^123. Correcting attribution as well, so that zero-point energy applies only to condensations that actually exist, collapses the calculation entirely, to the single expression:

$$\rho\_vac = \rho\_s * c^2 = 5.30 \text{ x } 10^{-10} \ J/m^3$$

with no additional constants and no fitting parameter beyond ρ_s and c, matching the observed value directly [P2].

An ocean illustrates the distinction the standard calculation fails to draw. An ocean has a bulk density and a bulk energy density at equilibrium; within it, waves can form, real, measurable disturbances with their own energy. The energy of the waves is not the same quantity as the bulk density of the ocean itself, and asking why the ocean's bulk density fails to equal the sum of all possible wave energies is a category-confused question. The standard QFT vacuum-energy calculation treats condensation-oscillation energy, the waves, as if it must equal the substrate's own bulk density, the ocean; the 10^121 discrepancy is the consequence of comparing two different physical categories as though they were competing estimates of the same one [P2].

Cosmic redshift is Doppler motion of receding matter under BFUT gravitational dynamics, with the photon propagating through a static, non-expanding substrate [P23]. The apparent cosmic acceleration attributed to dark energy in standard cosmology is consistent with observer bulk flow alone, with no requirement for either metric expansion or a separate dark-energy component [P4]. Because the substrate does not stretch, a photon's energy is fixed at the moment of emission, and the persistence domain L_persist described in Section 7 is evaluated once, at that emission energy, with no continuous recomputation during transit [P23].

9. Quantum Mechanics as Substrate Behaviour

The single-substrate picture extends to quantum mechanical phenomena usually treated as foundational and unexplained. The reduced Planck constant follows from condensation geometry instead of standing as a free constant of nature [P16, P27]:

$$\hbar = m\_p * c * r\_p / (\pi * R_0)$$

reproducing the measured value of ħ to within 0.0007%, as shown in the table in Section 5 [P16]. The physical reading is that the quantum of action is the action associated with one complete circulation of a substrate condensation at the condensation scale [P16, P27].

Once ħ is understood this way, the Born rule's characteristic squared-amplitude probability structure, half-integer spin, the Pauli exclusion principle, wavefunction collapse, superposition, and entanglement are each given a physical mechanism rooted in substrate dynamics instead of treated as separate postulates layered onto an abstract Hilbert space [P19A]. The same substrate structure that fixes ρ_s also fixes a fundamental decoherence floor, dissolving the usual incompatibility between quantum mechanics and gravity without requiring gravitons [P19A].

The Higgs field, often regarded as the most mysterious sector of the Standard Model, is one sector of the same Spaticle substrate, identified through a vacuum self-consistency condition structurally identical to the Higgs vacuum condition of the Standard Model. The Higgs mass follows as the geometric mean of the top quark and Z boson masses, m_H = sqrt(m_top * m_Z), giving approximately 125.51 GeV against a measured value of 125.25 GeV, an agreement of 0.21%, as shown in Section 5 [P19, P19A].

The same substrate framework extends to predictions for quantum computing hardware. Non-Markovian noise arising from substrate memory, preparation-history dependence of nominally identical quantum states, local matter distribution effects on qubit error rates, a scalability ceiling from substrate modular universality, tunnelling universality across material systems, a photonic-fermionic decoherence asymmetry, and a photon domain boundary specific to quantum hardware are all derived as direct, testable consequences of the same ρ_s and the same persistence-domain mechanism described in Section 7 [P24]. The detailed derivations and experimental proposals for these predictions are restricted by the author and are not reproduced here.

10. From Force to Sensing Channel: The Bridge to Consciousness

The chain traced through this paper does not stop at physics in the conventional sense. From the Spaticle field emerges matter, through the condensation functional of Section 5. From matter emerges the fundamental forces, through the mechanisms of Section 6. From those forces emerge the sensing channels through which physical systems detect and respond to their environment, and from sensing channels emerges the Hierarchical Channel Accessibility framework and the Consciousness Index developed in BFUT Papers 20 and 21 [P20, P21]. The four fundamental forces function as a hierarchy of sensing channels instead of as forces alone: gravity provides presence sensing, the strong force provides binding, electromagnetism provides identity and distance sensing, and the weak force provides transformation-threshold detection. Each force, already derived in Section 6 as a substrate phenomenon, is simultaneously a channel through which a physical system can detect and respond to some aspect of its environment; consciousness, in this framework, is a measurable physical phenomenon grounded in the accessible structure of these channels, not an independent property added on top of physics.

Paper 20 establishes a formal three-condition definition of sensing grounded in the same substrate framework established here, and develops the Hierarchical Channel Accessibility model linking channel structure, controlled emission, and structural inclusion to degree of consciousness [P20]. Paper 21 develops the Consciousness Index as a physically grounded scalar measure of conscious degree, structure, and evolutionary potential, derived from this same channel hierarchy [P21]. The detailed mechanisms of channel formation, the Consciousness Index itself, and their evolutionary implications are developed fully in those two papers and are not repeated here; this paper records only that the chain from substrate to consciousness is continuous and that each link in it is stated and cited at the point it is established.

11. Electric Fields, Magnetic Fields, and Photons as One Substrate Behaviour

A further unification, established directly from the Spaticle field's bound and free excitation structure, removes the conventional separation between static electromagnetic fields and propagating photons [P23]. Electric fields and magnetic fields are bound electromagnetic wave configurations: organised substrate excitations that remain attached to the source structure that generated them, forming a stable standing-wave or circulating-wave configuration instead of propagating away. Photons are the same kind of substrate excitation after detachment from the source, propagating freely through the medium at c up to their energy-dependent persistence domain described in Section 7 [P23]. The distinction that matters throughout the programme is not between real and virtual photons; it is between bound and free states of one substrate field [P23].

12. Conclusion

The evidence surveyed in this paper is organised by physical behaviour instead of by the sequence of papers that established it, and the pattern that emerges is the same regardless of how the material is grouped: one fixed substrate density, ρ_s = 5.9 x 10^-27 kg/m^3, accounts for the Hubble relationship, the cosmic microwave background, the Sunyaev-Zel'dovich and integrated Sachs-Wolfe effects, the lithium and S8 tensions, black hole structure, particle masses, galaxy rotation curves, weak gravitational lensing, atomic structure, matter stability, the cosmological constant, the Higgs mass, and the propagation behaviour of light and gravity, with no per-result adjustment anywhere in the chain.

The Spaticle field density is the primary physical quantity in this framework [P2]. Cosmic redshift is Doppler motion under BFUT gravitational dynamics [P23]. Both positions reinforce the central claim: the substrate is the foundation of the chain traced in this paper, not a quantity derived from any of its own consequences.

The chain traced here extends past the boundary of physics in the conventional sense, from substrate to matter, from matter to force, from force to sensing channel, and from sensing channel to the consciousness framework of Papers 20 and 21. The convergence documented in Section 4 is the strongest and most quantitatively constrained part of the programme; the consciousness framework is the newest and least independently tested. The claim of this paper is narrower and more specific than equal confidence in every step: that the same single substrate, and no other assumption, is the starting point of every step in the chain, and that this is recorded explicitly here so that the relationship between the programme's cosmological, physical, and biological results is visible in one place.

The papers cited throughout this synthesis fit into a broad architecture. Papers 1 through 13 establish the cosmological and observational foundations, reinterpreting the Hubble relationship, the cosmic microwave background, and related structure without metric expansion or dark energy. The present paper, Paper 14, synthesises the convergent evidence for the Spaticle field itself as the substrate underlying that cosmology. Papers 15 onward develop the consequences of that substrate in turn: the prior energy state preceding its manifestation, the emergence of matter and the fundamental forces, gravity, time and light, quantum mechanical behaviour, and the sensing-channel framework extending into consciousness, with the programme continuing to grow beyond the papers cited directly in this synthesis. This paper is intended to function as the primary entry point into that architecture for a reader approaching the programme for the first time.

Appendix A

The Spaticle Field Across All Results: Formula Reference (provided for reference in support of BFUT Paper 14)

Central anchor: one substrate density $\rho\_s = 5.9 \times 10^{-27}$ kg/m^3 governs every result in this paper.

Rows ordered from simplest (ρ_s direct) to most derived. standard model and QCD position.

Vs.what BFUT P16 derives from the Spaticle field.

#	Formula / Result	Standard model / GR / SR / QFT position	BFUT: what the Spaticle field derives	Formula / Value
LEVEL 1 - ρ_s appears directly				
1	Substrate density [Foundation]	No physical medium. The vacuum is geometric spacetime. Particle masses are input parameters of the Standard Model with no derivation from a common source.	The vacuum is a physically real substrate with an intrinsic equilibrium density. Every result below is a consequence of this one number existing.	$\rho\_s = 5.9 \times 10^{-27}$ kg/m³
2	Nucleation energy functional [P16 Sec. 3]	Quark confinement is described by QCD through the strong coupling constant α_s. The mechanism producing the first stable quark-class structure from a vacuum is not derived - the vacuum is assumed to contain virtual quark-antiquark pairs.	The first stable quark-class excitation nucleates from the Spaticle substrate. Its energy as a function of localisation radius R has an interior minimum.	$E(R) = A/R^2 + B \cdot R^2 + C \cdot R + D/R$. Minimum at $R_0 = 1.27348$
3	Quark condensation radius [P16 Sec. 4]	The proton charge radius r_p = 0.8414 fm is measured. Its geometric relationship to a quark radius is model-dependent and not derived from first principles in QCD.	The three-sphere packing geometry gives r_q exactly from r_p with no free parameters. One measured input. One derived output.	$r\_q = r\_p / (1 + 2/\sqrt{3}) = 0.8414 / 2.1547 = 0.3905$ fm
4	Interstitial volume fraction [P16 Sec. 10]	No equivalent. QCD does not derive an interstitial volume fraction from sphere packing geometry.	The interstitial region between three close-packed spheres has a fixed geometric volume fraction relative to the quark volume. This is a pure geometric constant.	$V\_gap / V\_q = (2 \cdot \sqrt{3} - \pi) / (4 \cdot \pi/3) = 0.0770$
LEVEL 2 - one step from ρ_s: E_unit and the connecting identity				
5	Energy unit [P16 Sec. 4]	The proton mass m_p = 938.272 MeV is a measured input of the Standard Model. It is not derived from a	At the actual ρ_s, m_p is the measured SI anchor. The energy unit follows directly. A universe with different ρ_s	$E\_unit = m\_p \cdot c^2 / \pi = 298.661$ MeV (m_p is the measured anchor)

#	Formula / Result	Standard model / GR / SR / QFT position	BFUT: what the Spaticle field derives	Formula / Value
		substrate density or geometric principle.	would have a different E_unit scaling proportionally.	
6	Electron mass - connecting identity [P16 Sec. 10]	The electron mass m_e = 0.511 MeV is a measured parameter of the Standard Model. Its ratio to the proton mass m_e/m_p = 1/1836 is known but not derived from any geometric principle.	The electron mass follows from the interstitial geometry alone. E_unit cancels from both sides. The ratio m_e/m_p = $1/(6\cdot\pi^5)$ is a pure geometric constant independent of ρ_s.	E_gap / m_e = $6\cdot\pi^4\cdot$V_gap/V_q = 45.00 [exact]. m_e = E_unit/$(6\cdot\pi^4)$ = 0.511009 MeV. m_e/m_p = $1/(6\cdot\pi^5)$ [geometry only]
7	Interstitial gap energy [P16 Sec. 10]	No equivalent in QCD or the Standard Model.	The gap energy is the condensation energy of the interstitial substrate volume. It is the physical energy available for electron creation.	E_gap = E_unit · V_gap/V_q = 298.661 · 0.0770 = 22.999 MeV
LEVEL 3 - two steps from ρ_s: threshold, 3+e, proton formation				
8	Three-core energy [P16 Sec. 6]	QCD describes three-quark binding through gluon exchange. The binding energy of a proton is approximately -939 MeV relative to free quarks. The mechanism is perturbative and non-perturbative QCD.	Three co-rotating substrate units form the first stable cooperative core. Energy computed directly from the condensation functional.	E(3-core) = 0.900 model units (full five-term functional, J=1.0, lam=0.6, α=0.5, D_s=1.5)
9	N=3+1 partition energy comparison [P16 Sec. 6]	QCD does not derive a partition energy comparison between symmetric and asymmetric quark arrangements from a free-energy functional.	At n=4 total units, partition energies confirm which arrangement is preferred. N=3+1 decisively preferred over 4+0 and 2+2. This is a calculational result, not the physical proton.	4+0 = 4.60. 2+2 = 4.00. N=3+1 = 1.40 [preferred] (all model units)
10	3+e state - proton formation [P16 Sec. 10]	The proton is a bound state of three quarks in QCD. The mechanism producing exactly three quarks with specific charge assignments is the Standard Model's assignment of quark quantum numbers, not a derivation.	The three-core generates its own electron through the 3+e mechanism. Energy drops from 0.900 to 0.8958. This is the physical proton-class structure. The electron is not a separate entity - it is created by the three-core.	E(3+e) = 0.8958 model units. ΔE = 0.0042 model units
11	Robustness of 3+e threshold [P16 Sec. 6.1]	QCD predicts proton stability through colour confinement. The stability is absolute within QCD - no parameter scan is used to establish it.	The 3+e preference holds across 97.56% of 1D, 95.95% of 2D, and 90.43% of 3D parameter space. Not a fragile result at a single tuned point.	1D: 97.56%. 2D: 95.95%. 3D: 90.43% (full five-term functional)
LEVEL 4 - matter-antimatter, forces, and hydrogen				
12	Stability filter and antimatter [P16 Sec. 7-9]	Matter-antimatter asymmetry is attributed to CP violation in the Standard Model. The Sakharov conditions require baryon number violation, CP violation, and departure from thermal equilibrium. No single mechanism produces both matter and antimatter from the same process.	The stability filter operates at formation. 90-97% of excitations stabilise as 3+e (matter). The remaining 2-10% are unstable excitations that collapse. The rebound is what physics calls the antiparticle. Antimatter is not an independently stable population; it is the cancellation wave of a failed excitation.	Stable 3+e (matter): 90-97%. Unstable collapse: 2-10%. Annihilation: complete (topology cancels exactly)

#	Formula / Result	Standard model / GR / SR / QFT position	BFUT: what the Spaticle field derives	Formula / Value
13	Matter-antimatter annihilation [P16 Sec. 8]	Matter-antimatter annihilation is described by QED and QCD via conservation of quantum numbers. The physical mechanism of why annihilation must be complete is not derived from first principles.	Matter and antimatter are circulation-topology inverses of the same substrate solution. When they meet, the circulations cancel exactly. Annihilation is geometrically complete because the topologies are exact inverses.	3+e topology: (co-rotate, co-rotate, co-rotate). Inverse topology: (counter, counter, counter). Cancellation: exact by geometry
14	Force preconditions from 3+e topology [P16 Sec. 2, 15]	The four fundamental forces are described by separate theories: QCD (strong), QED (electromagnetic), electroweak theory (weak), GR (gravity). No single mechanism derives all four from one substrate topology.	The 3+e topology establishes the physical preconditions for all four forces. Charge separation between three-core and generated electron: precondition for electromagnetic force. Three-sphere packing geometry: precondition for strong confinement. Stability filter asymmetry: precondition for weak force asymmetry. Substrate deformation: precondition for gravity.	EM: charge separation in 3+e. Strong: three-sphere confinement. Weak: stability filter asymmetry. Gravity: substrate deformation (preconditions; see Levels 6-7 for the full derivation)
15	Hydrogen ground state - Bohr radius [P16 Sec. 11]	The Bohr radius a_0 = 52,918 fm is derived from QED using the measured electron mass and fine structure constant. It is not derived from a substrate density.	The Bohr radius follows from the electron mass which follows from the connecting identity which follows from ρ_s. A universe with different ρ_s would have atoms of different size.	$a_0 = \hbar^2/(m_e \cdot k_e \cdot e^2)$ = 52,918 fm. a_0 proportional to ρ_s^{-1}
16	Hydrogen binding energy [P16 Sec. 11]	The hydrogen ground state energy -13.6 eV is derived from QED. It is not connected to a substrate density.	The binding energy follows from m_e which follows from ρ_s. A universe with different ρ_s would have different atomic binding energies.	E_H = -13.6 eV = $-m_e \cdot k_e^2 \cdot e^4/(2 \cdot \hbar^2)$. E_H proportional to ρ_s
LEVEL 5 - grand implication: modularity and the universality of hierarchy				
17	Modular organisation principle [P16 Sec. 12]	Hierarchy in nature (quarks to nucleons to atoms to molecules to cells to galaxies) is treated as an observed feature requiring separate explanations at each scale. No single principle derives hierarchy from energy minimisation.	The condensation functional shows that repeated reuse of the 3+e module is energetically preferred over continued monolithic growth at clean multiples of three units. The energy advantage at clean multiples grows with system size.	E_{single} grows superlinearly. $E_{modular} = \mathrm{floor}(n/3) \cdot 0.8958 + E_{remainder}$. Gap grows at clean multiples
18	Particle identity and finite catalogue [P16 Sec. 12]	All electrons are identical by quantum field theory - they are excitations of the same universal field. The number of stable particles is an experimental observation. No derivation of why exactly these particles are stable is offered.	Identical particles are repeated realisations of the same stable substrate solution. The finite particle catalogue follows from the finite number of deep minima in the substrate free-energy landscape. At n=4 exactly three configurations exist; 3+e dominates.	$m_e/m_p = 1/(6 \cdot \pi^5)$ [pure geometry, ρ_s cancels]. Stable configurations at n=4: 3+e: 97.56%. 2+2: 2.16%. 4+0: 0.28%
19	Atom size fixed by ρ_s [P16 App. C]	The atomic scale is set by the Bohr radius which uses measured constants. No derivation of why atoms are the specific size they are is offered in standard physics.	Atom size is a derived consequence of ρ_s. If ρ_s doubled, atoms would be half the size. The actual atom size follows from the substrate	m_p proportional to ρ_s. m_e proportional to ρ_s. a_0 proportional to ρ_s^{-1}. E_H proportional to ρ_s. m_e/m_p = constant [geometry]

#	Formula / Result	Standard model / GR / SR / QFT position	BFUT: what the Spaticle field derives	Formula / Value
			density through the connecting identity chain.	
LEVEL 6 - forces emerge from the 3+e topology [P17]				
20	Gravity as substrate restoring response [P17 Sec. 2-3]	GR: gravity is geometric curvature of spacetime sourced by mass-energy. No mechanical mechanism is given for why mass curves spacetime.	Gravity is the Spaticle substrate's own mechanical restoring response to deformation by mass, instead of an externally imposed geometric feature. Connects directly to the covariant carrier equation validated in P18.	Mechanism derived in P17; quantitative carrier equation in P18 (Level 7)
21	Strong-force confinement potential [P17 Sec. 5.2 / P19 Sec. 20.6]	QCD: confinement modelled through colour charge and gluon exchange. The string tension (~0.9 GeV/fm) is measured, not derived from a substrate.	A three-term potential, overlap attraction plus hard-core repulsion plus linear confinement, derived entirely from ρ_s, r_p, and the P16 condensation geometry. No new free parameters.	$C_s = F_{conf} = 0.574$ GeV/fm vs measured 0.9 GeV/fm. Difference: 36%
22	Fine structure constant from circulation asymmetry [P17 Sec. 6.8 / P19]	QED: $\alpha = 1/137.036$ is measured; no physical mechanism derives its value.	$\alpha = e^2 / (4 \cdot \pi \cdot \varepsilon_0 \cdot \hbar \cdot c)$, with $\hbar = m_p \cdot c \cdot r_p / (\pi \cdot R_0)$ substituted from the P16 condensation geometry.	$\alpha_{BFUT} = 1/137.037$ vs 1/137.036. Difference: 0.00048%
23	Weak mixing angle and parity violation [P17 Sec. 7.3 / P19 Sec. 6]	Electroweak theory: $\sin^2(\theta_W) = 0.2312$ is measured. Parity violation is an input symmetry choice, not derived from a mechanism.	$\sin^2(\theta_W)$ is derived from the bifurcation chirality angle of the 3+e formation; parity violation follows from the fixed counter-rotation handedness of the generated electron unit.	$\sin^2(\theta_W) = 0.2312$ vs 0.2312 measured. Difference: 0.01% [per Master Symbol Guide]
24	Electron-capture / neutron-formation threshold [P17 Sec. 7.4D]	Standard Model: electron-capture threshold 0.782 MeV = $(m_n - m_p - m_e)c^2$ is measured; not connected to a substrate mechanism.	The threshold is the dominance-inversion point at which the electron unit's rotational energy density exceeds the three-core's rest-mass substrate deformation, set by ρ_s, r_p, and the expelled mass fraction mu.	0.782 MeV (dominance-inversion threshold)
LEVEL 7 - unified gravitation, rotation curves, and gravitational waves [P18]				
25	Covariant carrier field equation, F1-cov [P18 Sec. 3]	GR: curvature sourced by the stress-energy tensor with instantaneous-limit response. Newtonian gravity: action treated as instantaneous.	A single covariant carrier equation with a finite response time τ_c. GR and Newtonian gravity are recovered as settled-domain approximations as $\tau_c \to 0$.	$\tau_c \cdot d\Psi/dt + \Psi - L_{rlx}^2 \cdot \nabla^2 \Psi = K \cdot J[T_{mn}]$ (F1)
26	Carrier relaxation timescale [P18]	GR / Newtonian gravity: no relaxation time; gravitational response is instantaneous (Newtonian limit) or exactly luminal (GR).	A finite carrier response time, derived from ρ_s alone, with no free parameters.	$\tau_c = 1/(c \cdot \sqrt{3 \cdot \rho_s})$, $L_{rlx} = c \cdot \tau_c$
27	Finite gravitational domain radius, DDR [P18]	Lambda-CDM: dark matter halo profile (e.g. NFW) fitted per galaxy with two or more free parameters.	Every mass has a finite deformation domain set by ρ_s; rotational entrainment adds support at large radii with no per-galaxy tuning.	$R_d = (3M/(8 \cdot \pi \cdot \rho_s))^{(1/3)}$. $R_{eff} = R_d \cdot (1+v_{rot}^2/c^2)^{(1/3)}$

#	Formula / Result	Standard model / GR / SR / QFT position	BFUT: what the Spaticle field derives	Formula / Value
28	175 SPARC galaxy rotation curve validation [P18]	Lambda-CDM/NFW: χ^2 fitted per galaxy with free halo parameters. MOND: $\chi^2 = 1.47$ with a single universal acceleration scale.	Shape agreement 86.3% (flat correct 93.0%, non-flat correct 27.8%) across all 175 SPARC galaxies from a single ρ_s, with no per-galaxy tuning.	BFUT shape agreement 86.3% (DM1 entrainment formula), no free parameters
29	KiDS-1000 weak gravitational lensing [P18]	Standard NFW halo profile: χ^2 = 5.77 to 6.57 across four stellar-mass bins, with halo concentration and virial mass fitted independently per bin.	The same ρ_s and domain profile used for rotation curves, with no free parameters, independently confirms the substrate density.	χ^2_BFUT = approximately 2 to 3 (DM2 entrainment formula) vs χ^2_NFW = 5.77-6.57
30	Carrier relaxation as a structural prediction [P18]	GR: ringdown described fully by quasi-normal modes; no residual decay channel tied to a substrate is predicted.	An observable carrier residual decaying at τ_c, scaled by a mass/compactness enhancement factor F >= 1 above the vacuum floor.	$\tau\_obs = F \times \tau\_c$, F >= 1
31	Spaticle field as the physical referent of "dark matter" [P18]	Lambda-CDM: dark matter is a particulate substance, undetected directly after decades of dedicated search programmes.	The operational properties required of dark matter, gravitational effect without luminosity, halo-like spatial profile, no direct particle signal, are all satisfied by the real Spaticle substrate. The detection programme has been measuring substrate effects under the wrong ontological label.	A single ρ_s reproduces rotation curves and lensing simultaneously
LEVEL 8 - dark matter identification by coherence index [P25]				
32	DDR Coherence Index [P25, building on the P18 DDR domain equation]	Lambda-CDM: dark matter content inferred statistically per system via N-body-calibrated halo fitting.	A single formula predicts the outer rotation velocity of a disk galaxy from its baryonic mass and characteristic speed, using global constants shared across the sample, not fitted per galaxy.	M_extra(<R) = $4\pi \cdot \rho\_s \cdot A \cdot (M\_bar/10^{10} M_\odot)^\alpha \cdot f(V\_char) \cdot R\_ref^2 \cdot R \cdot \xi(R)$; $V\_pred^2 = V\_bar^2 + G \cdot M\_extra/R$. A=2500, α=0.5, R_ref=15 kpc
33	Validation across 175 SPARC galaxies and 190 systems to z=4.26 [P25]	Lambda-CDM: ultra-diffuse and anomalously low-dark-matter galaxies are treated as active research and model-refinement cases.	Shape agreement across the full SPARC sample, and validation across additional systems spanning z=0 to z=4.26, all with the same global constants.	175/175 SPARC galaxies tested, shape agreement 86.3%, flat correct 93.0%, non-flat correct 27.8%. Global constants A=2500, α=0.5
LEVEL 9 - time and relativity from a propagation budget [P22]				
34	Special-relativistic time dilation [P22]	SR: the Lorentz factor is postulated from the constancy of c; no physical mechanism is given for why clocks slow.	Derived from a finite propagation budget shared between spatial motion and internal state evolution of the substrate.	$c^2 = v\_spatial^2 + v\_internal^2$ => $\eta = \sqrt{1 - v^2/c^2}$
35	Gravitational time dilation [P22]	GR: time dilation is a geometric consequence of spacetime curvature; the same mathematical form as kinematic dilation, but with no unifying physical cause given for both.	Mass-energy deforms the substrate, reducing local propagation efficiency η; the same reduction lowers clock rates and local propagation speed together, by the same factor as kinematic dilation.	$\eta(r)$ tied to the same R_d domain function derived in P18
36	Universal speed limit as a causal bound [P22]	SR: c is postulated as an absolute speed limit; the	c is the maximum rate at which the substrate can reorganise itself; no causal	c_0 = maximum substrate reorganisation rate (explicit formula in P23, Level 10)

#	Formula / Result	Standard model / GR / SR / QFT position	BFUT: what the Spaticle field derives	Formula / Value
		reason for its universality is not derived.	influence can propagate faster than that rate.	
LEVEL 10 - light, photons, and the universal speed limit [P23]				
37	Speed of light from substrate stiffness and density [P23 Sec. 2]	SR/QED: $c = 2.997925 \times 10^8$ m/s is measured; treated as fundamental, not derived from a medium.	c is the propagation speed of the Spaticle substrate, set by its stiffness-to-density ratio.	$c = \sqrt{K_s/\rho_s}$. $K_s = \rho_s \cdot c^2 = 5.30 \times 10^{-10}$ Pa
38	Cross-check of c from independent BFUT constants [P23]	SR: c is independently measured and not cross-checked against any other derived constant.	c reconstructed from e, R_0, ε_0, m_p, r_p, and α, all fixed independently elsewhere in the programme.	$c = \sqrt{e^2 \cdot R_0/(4 \cdot \varepsilon_0 \cdot m_p \cdot r_p \cdot \alpha)}$. Difference from measured: 0.0003%
39	Velocity deficit of massive particles [P23]	SR: massive particles approach but never reach c; the reason is expressed kinematically, not physically.	Part of a massive particle's energy budget is committed to maintaining its condensation structure instead of propagation. The deficit from c is set by the ratio of rest energy to total energy.	$v/c = pc/E = pc/\sqrt{(pc)^2+(mc^2)^2}$. Neutrinos within 1 part in 10^{-17} of c
40	Equivalence of light speed and gravitational wave speed [P23]	GR/QED: light and gravitational waves both travel at c; treated as two independently confirmed facts instead of one derived consequence.	Light and gravitational waves are both organised disturbances of the same substrate of density ρ_s and stiffness K_s, so both necessarily propagate at the same speed.	$c_{light} = c_{GW} = \sqrt{K_s/\rho_s}$, a structural consequence of one substrate carrying both disturbances
LEVEL 11 - the Planck constant and quantum mechanics [P27]				
41	Reduced Planck constant from condensation geometry [P27 Sec. 2]	QM: $\hbar = 1.054571 \times 10^{-34}$ J·s is measured; treated as a fundamental postulate.	ħ follows from the P16 condensation geometry, anchored only by the independently measured proton charge radius r_p.	$\hbar = m_p \cdot c \cdot r_p/(\pi \cdot R_0)$. Difference: 0.0007%
42	Compton wavelength, de Broglie wavelength, spin-1/2 angular momentum [P27]	QM: these formulas take ħ as an input constant with no link to a substrate geometry.	Each follows directly from substituting the BFUT ħ expression into the standard formula.	Compton: $m_p \cdot r_p/(\pi \cdot R_0 \cdot m)$. Spin-1/2: $m_p \cdot c \cdot r_p/(2 \cdot \pi \cdot R_0)$. Difference: 0.0007% (uniform across particles)
43	Planck length, mass, and time [P27 Sec. 12]	QM/GR: Planck units combine ħ, G, and c as independent fundamental constants with no further reduction.	All three reduce to the same R_0 and ρ_s-anchored chain as ħ; each is a geometric mean of the condensation scale and a gravitational scale.	$l_P = \sqrt{m_p \cdot r_p \cdot G/(\pi \cdot R_0 \cdot c^2)}$. $m_P = \sqrt{m_p \cdot c^2 \cdot r_p/(\pi \cdot R_0 \cdot G)}$. $t_P = \sqrt{m_p \cdot r_p \cdot G/(\pi \cdot R_0 \cdot c^4)}$. Difference: 0.0003% (all three)
44	Vacuum (zero-point) energy density [P27]	QFT: zero-point energy of empty field modes; the basis of the $\sim 10^{122}$ discrepancy against the observed cosmological constant.	Zero-point energy is a property of organised condensations instead of empty field modes; this reframing yields the substrate vacuum energy density directly, with no discrepancy.	$\rho_{vac} = \rho_s \cdot c^2 = 5.3 \times 10^{-10}$ J/m³ (intrinsic substrate property)
45	Spin-statistics theorem [P27]	QM: the spin-statistics connection (integer spin = bosons, half-integer spin = fermions) is a postulate confirmed within QFT, not derived from geometry.	Derived from the 720-degree versus 360-degree embedding topology required to restore the condensation to its original configuration.	720 degrees (fermion) vs 360 degrees (boson) restoration topology
LEVEL 12 - black holes as vortical compression cores [P28]				

#	Formula / Result	Standard model / GR / SR / QFT position	BFUT: what the Spaticle field derives	Formula / Value
46	Black hole replaced by a finite compression core [P28 Sec. 2]	GR: black holes are objects with a true central singularity and an event horizon.	What is observed as a black hole is a vortical compression core, a finite-density structure sustained by rotational dynamics in the Spaticle substrate. No singularity, no true horizon.	Four-region finite-core architecture replaces singularity plus horizon
47	Domain radius and seed dissipation timescale [P28 Sec. 3.4]	GR: no equivalent concept; a formed black hole is permanent by definition.	A seed core not continuously reinforced by rotational inflow dissipates on a finite timescale set by ρ_s.	$R\_d = (3M/(8\cdot\pi\cdot\rho\_s))^{(1/3)}$. $\tau\_dissip = R\_d/c$. 10 M_sun isolated seed: ~59 minutes
48	Rotational Sustenance Principle and Threshold [P28 Sec. 3.4]	GR: persistence of a black hole requires no ongoing physical process beyond its initial formation.	No vortical compression core can persist without continuous rotational reinforcement. The Rotational Sustenance Threshold is the condition under which reinforcement exceeds dissipation within τ_dissip.	Threshold condition: $C > C\_crit$ within $\tau\_dissip = R\_d/c$
49	Universal Centrality Rule [P28 Sec. 5]	GR: a black hole's position at the centre of its host system is an observational regularity without a structural derivation.	Every vortical core occupies the exact dynamical centre of its host system, as a structural consequence of the formation pathway instead of coincidence.	Centrality follows directly from the rotational-aggregation formation pathway
50	Hawking radiation has no physical realisation [P28]	Standard physics: Hawking radiation is a theoretical prediction of black hole evaporation via vacuum particle-pair production at the horizon.	All five foundational premises required for Hawking radiation, including a true horizon and a true vacuum at the horizon, describe conditions that do not exist in a Spaticle substrate universe.	No physical realisation under BFUT; replaced by finite-core thermodynamics

References

[1] Einstein, A. (1920). Ether and the Theory of Relativity. Address delivered at the University of Leiden, 5 May 1920. English translation by G. B. Jeffery and W. Perrett, in Sidelights on Relativity (1922), pp. 3-24. London: Methuen. Available via MacTutor History of Mathematics (mathshistory.st-andrews.ac.uk/Extras/Einstein_ether) and Project Gutenberg (gutenberg.org/ebooks/7333).

[P1] Sharma, V. S. (2026). Gravitational Sorting as an Alternative Mechanism for the Hubble Relationship. BFUT Paper 1. Zenodo. DOI: 10.5281/zenodo.19226423

[P2] Sharma, V. S. (2026). The Physical Identity of the Cosmological Constant. BFUT Paper 2. Zenodo. DOI: 10.5281/zenodo.19242083

[P3] Sharma, V. S. (2026). A Steady-State Nucleosynthesis Resolution of the Cosmological Lithium Problem. BFUT Paper 3. Zenodo. DOI: 10.5281/zenodo.19205920

[P4] Sharma, V. S. (2026). Observer Bulk Flow as an Alternative Explanation for Apparent Cosmic Acceleration. BFUT Paper 4. Zenodo. DOI: 10.5281/zenodo.19228065

[P5] Sharma, V. S. (2026). The Universe Has No Boundary: Logical, Derivational, and Observational Arguments for Spatial Infinitude. BFUT Paper 5. Zenodo. DOI: 10.5281/zenodo.19242759

[P6] Sharma, V. S. (2026). Black Holes as Central Gravitational Vortices Lacking Singularities: The Universal Centrality Rule. BFUT Paper 6. Zenodo. DOI: 10.5281/zenodo.19300874

[P7] Sharma, V. S. (2026). Dynamic Thermal Equilibrium as an Alternative Origin for the CMB Temperature. BFUT Paper 7. Zenodo. DOI: 10.5281/zenodo.19302025

[P8] Sharma, V. S. (2026). Cold, Dark, and Inevitable: A Logical Reconstruction of the Universe Before the Big Flare-Up. BFUT Paper 8. Zenodo. DOI: 10.5281/zenodo.19323579

[P9] Sharma, V. S. (2026). Cosmic Rotation Across Scales, Emergent Orbital Hierarchy, and the Large-Scale Challenge to Metric Expansion. BFUT Paper 9. Zenodo. DOI: 10.5281/zenodo.19341549

[P10] Sharma, V. S. (2026). The Sunyaev-Zel'dovich Effect as Local Substrate Interaction: A Big Flare-Up Theory Reinterpretation. BFUT Paper 10. Zenodo. DOI: 10.5281/zenodo.19377396

[P11] Sharma, V. S. (2026). The Lyman-Alpha Forest in the Big Flare-Up Theory: Absorption Percolation Threshold. BFUT Paper 11. Zenodo. DOI: 10.5281/zenodo.19383804

[P12] Sharma, V. S. (2026). The Integrated Sachs-Wolfe Effect in BFUT: Local Spaticle Field Temperature Variations as an Alternative Origin. BFUT Paper 12. Zenodo. DOI: 10.5281/zenodo.19391470

[P13] Sharma, V. S. (2026). Weak Gravitational Lensing and the S8 Tension in BFUT: Why Late-Time Clustering Inference Is Not a Unique Test of Lambda-CDM. BFUT Paper 13. Zenodo. DOI: 10.5281/zenodo.19392597

[P14] Sharma, V. S. (2026). The Spaticle Field as the Unified Substrate of Physical Reality: A Cross-Programme Synthesis of Convergent Evidence, From Cosmology and Particle Masses to Consciousness. BFUT Paper 14. Zenodo. DOI: 10.5281/zenodo.19394064

[P15] Sharma, V. S. (2026). What Existed Before Matter and the Spaticle Field: The Origin of Space, Time, and the Physical Substrate of Reality in an Infinite Universe. BFUT Paper 15. Zenodo. DOI: 10.5281/zenodo.19811691

[P16] Sharma, V. S. (2026). The Origin of Matter, Antimatter, and Fundamental Forces: How Protons, Electrons, and Hydrogen Formed. BFUT Paper 16. Zenodo. DOI: 10.5281/zenodo.19908215

[P17] Sharma, V. S. (2026). The Emergence of Forces and Fundamental Senses: How the Spaticle Field Gave Rise to Gravity and All Other Forces. BFUT Paper 17. Zenodo. DOI: 10.5281/zenodo.19976408

[P18] Sharma, V. S. (2026). Beyond General Relativity: A Unified Gravitation Equation Across Quantum, Classical, Galactic, and Cosmological Scales. BFUT Paper 18. Zenodo. DOI: 10.5281/zenodo.20145506

[P19] Sharma, V. S. (2026). Unification of Particle Physics: Deriving Fine Structure and Coupling Constants, W, Z, and Higgs Boson Masses. BFUT Paper 19. Zenodo. DOI: 10.5281/zenodo.20145567

[P19A] Sharma, V. S. (2026). Unifying Quantum Mechanics with Gravity, Demystifying Twenty Quantum Phenomena Including Half-Integer Spin, the Born Rule, Wave Function Collapse, and Higgs Physics. BFUT Paper 19A. Zenodo. DOI: 10.5281/zenodo.20145695

[P20] Sharma, V. S. (2026). From Matter and Fundamental Forces to Consciousness: A Unified Framework of Sensing Channels, Control, and Evolution. BFUT Paper 20. Zenodo. DOI: 10.5281/zenodo.19992457

[P21] Sharma, V. S. (2026). The Consciousness Index (CI): A Physically Grounded Scalar Measure of Conscious Degree, Structure, and Evolutionary Potential. BFUT Paper 21. Zenodo. DOI: 10.5281/zenodo.20025739

[P22] Sharma, V. S. (2026). Time: Identifying the Cause and Effects and Unifying General and Special Relativity. BFUT Paper 22. Zenodo. DOI: 10.5281/zenodo.20556908

[P23] Sharma, V. S. (2026). Light, Photons, and the Universal Speed Limit: A First-Principles Derivation of c from Substrate Condensation Dynamics. BFUT Paper 23. Zenodo. DOI: 10.5281/zenodo.20577935

[P24] Sharma, V. S. (2026). Quantum Computing and the Missing Physics Causing Delays and Overspend: Real Unknown Unknowns Identified Through the BFUT Substrate Framework. BFUT Paper 24. Zenodo. DOI: 10.5281/zenodo.20620192. Access to the full derivations and experimental proposals in this paper is restricted by the author.

[P25] Sharma, V. S. (2026). Dark Matter: Connecting Galaxy Clusters, Galaxy Rotations, the Cosmological Constant, W and Z Boson Masses, and Atomic Structure Through One Physical Constant. BFUT Paper 25. Zenodo. DOI: 10.5281/zenodo.20535295

[P26] Sharma, V. S. (2026). Singularity: Why and How Physical Substrate Dynamics Make Infinite Density Impossible. BFUT Paper 26. Zenodo. DOI: 10.5281/zenodo.20557070

[P27] Sharma, V. S. (2026). The Planck Constant: A First-Principles Derivation of ħ and How It Reshapes the Interpretation of Quantum Mechanics. BFUT Paper 27. Zenodo. DOI: 10.5281/zenodo.20620283